Supporting Information for:

Top-down modulation of sensory cortex gates perceptual learning

Melissa L. Caras[a,1], Dan H. Sanes[a,b,c]

This PDF file includes:

Materials and Methods

Supplementary References

Figs. S1 to S14

Tables S1 to S4

Materials and Methods

Subjects

Adult Mongolian gerbils (*Meriones unguiculatus*) were raised from commercially obtained breeding pairs (Charles River). Animals were housed on a 12-h light/12-h dark cycle, and provided with *ad libitum* food and water unless otherwise noted. All procedures were approved by the Institutional Animal Care and Use Committee at New York University.

Behavioral Apparatus

Behavioral performance was assessed with a yes-no aversive conditioning paradigm, as described previously (1-5). Briefly, a stainless steel spout was positioned above a metal floorplate within a test cage. Water delivery was initiated by a syringe pump (NE-1000; New Era Pump Systems) triggered by infrared detection at the spout contact. Sound stimuli were delivered from a calibrated free-field speaker (DX25TG05-04; Vifa) positioned 1m in front of the test cage. The cage and speaker were housed within a sound-attenuating room (GretchKen), and monitored remotely. Stimulus delivery and data acquisition were controlled using custom Python scripts (written by Dr. Bradley Buran) and an RZ6 multifunction processor (Tucker Davis Technologies).

Associative Training

Animals were placed on controlled water access, and trained to drink continuously while in the presence of steady, unmodulated, broadband noise (60 dB SPL; 2.5-20 kHz; 12 dB/octave roll-off). Animals learned to withdraw from the spout when the sound changed from the "safe" cue (unmodulated noise) to the "warn" cue (0 dB re: 100% depth sinusoidal AM noise; 5 Hz

modulation rate; 1 s duration) by pairing the warn cue with a mild shock (0.5-1.0 mA, 300 ms; Lafayette Instruments) delivered through the metal lick spout (Fig. 1A). To be consistent with previous literature, and because the decision axis for AM detection is logarithmic (6), depths are presented here on a dB scale (re: 100% depth). Thus, 0 dB (re: 100% depth) refers to fully modulated (100% depth) noise, and negative numbers refer to shallower depths. These dB (re:100% depth) values are not to be confused with dB SPL values, which indicate the root-mean-squared intensity of the stimulus.

Individual animals vary in their sensitivity to pain (7); thus, the shock level was adjusted on a subject-by-subject basis to reliably elicit spout withdrawal, without dissuading the animal from resuming drinking shortly thereafter. Warn trials were interspersed with 3-5 safe trials, during which the unmodulated sound continued unchanged. The unpredictable nature of the warn presentation prevented temporal conditioning. The gain of the AM signal was adjusted to control for changes in average power across modulation depths (6, 8).

Behavioral Scoring

Behavioral responses were scored by monitoring the animal's contact with the spout during the final 100 msec of each trial. Breaking contact for ≥ 50 msec was considered a spout "withdrawal" and was scored as a correct "hit" on warn trials (AM noise), and as an incorrect "false alarm" on safe trials (unmodulated noise; Fig. 1A). Testing began only after an animal had reached a criterion level of behavioral performance ($d' \geq 1.5$ for 0 dB depth; see Psychometric Analysis below). On the final day of associative training, and throughout testing, the root-mean-squared stimulus intensity was held constant at 45 dB SPL.

47 Psychometric Training and Testing

48 Each psychometric session began with a series of "reminder trials" at 0 dB depth. After the
49 animal responded correctly to 3 consecutive reminder stimuli (or consumed 0.5 mL of water,
50 whichever came first), psychometric assessment commenced. Five AM depths (Figs. S2-S3)
51 were presented in descending order (interspersed with 3-5 safe trials, as described above).

52 Animals underwent perceptual training for 5-14 days. Sessions took place every 24 to 48
53 hours. The five depths presented during the first psychometric session (0, -3, -6, -9 and -12 dB
54 re: 100%) were chosen because they bracketed naive AM depth detection thresholds, as
55 determined previously (2, 3, 5). The five AM depths presented in each subsequent session were
56 determined by the animal's performance on the previous day. Consecutive AM depths were
57 always in increments of 3 dB.

58 Maintaining threshold bracketing within and across sessions made it likely that animals
59 would fail to detect the smallest of the AM depths presented. Delivering shocks during such
60 trials would likely lead to a cessation of drinking, or intermittent pecking at the spout, which
61 would result in an excessively high false alarm rate. To avoid these possibilities, the shock was
62 turned off for the lowest two depths presented. A previous study (9) validated the necessity of
63 this approach, and confirmed that animals do not become conditioned to the presence or absence
64 of the shock.

65

66 Psychometric Analysis

67 The percent of "yes" responses (spout withdrawals) was plotted as function of modulation
68 depth. These psychometric functions were fit with a cumulative Gaussian using the maximum

likelihood procedure of the open-source package psignifit 4 for MATLAB (10). The formula for this function is as follows:

$$\Psi(x,m,w,\gamma,\lambda) = \gamma + (1-\gamma-\lambda)S(x;m,w) \quad (1)$$

where

$$S(x;m,w) = \Phi\left(C\frac{(x-m)}{w}\right) \text{ and } C = \Phi^{-1}(0.95) - \Phi^{-1}(0.5) \quad (2)$$

Here, Φ and Φ^{-1} represent the cumulative standard normal distribution and its inverse, x represents the modulation depth, m the threshold, λ the lapse rate, γ the false alarm rate, and w the width of the interval over which $S(x;m,w)$ rises from γ to λ.

Bayesian inference was used to obtain parameter estimates for a beta-binomial model; thus prior distributions were required for each parameter described above, as well as an additional parameter, η, which represents overdispersion. We used the default priors in Psignifit 4, which worked well for fitting our data. Thus, for m and w, uniform prior distributions were generated automatically from the x values in our dataset, and the prior distributions for γ, λ, and η were defined as beta-distributions with the parameters (1,10) (10).

Fits were transformed to the signal detection metric d' (11):

$$d' = Z(h) - Z(fa) \quad (3)$$

Here, h and fa represent the hit rate and false alarm rate, respectively. To avoid d' values that approach infinity, we set a floor (0.05) and ceiling (0.95) on hit rates and false alarm rates. For each psychometric fit, threshold was defined as the AM depth at which $d' = 1$, unless otherwise stated.

Electrode Implantation Surgery

Animals (n = 4 males) were anesthetized with isoflurane/O_2 and secured in a stereotaxic device (Kopf). An incision was made along the midline, and the skin and fascia were removed. The skull was exposed and dried with H_2O_2. Bone screws were inserted into both frontal bones and the right parietal bone. A craniotomy was made in the left parietal bone, dorsal and medial to auditory cortex. A 4 shank silicone probe array with 16 channels arranged in a 600 x 600 μm grid (A4x4-4mm-200-200-1250-H16_21mm; NeuroNexus) was fixed to a custom-made microdrive to allow for subsequent advancement, and angled 25 degrees in the mediolateral plane. The rostral-most shank of the array was positioned 3.9 mm rostral and 4.8 mm lateral to lambda, and inserted into left core auditory cortex (Fig. S13). Left auditory cortex was targeted because of its sensitivity to time-varying signals, including vocalizations, relative to the right hemisphere (12-14). A ground wire was inserted in the right caudal hemisphere, and the apparatus was secured to the skull via dental acrylic. Animals were allowed to recover for at least 1 week before being placed on controlled water access.

Neurophysiology

Recordings were made in awake animals before, during, and after behavioral sessions using previously described methodology (15, 16). Briefly, extracellular single- and multi-unit activity

was acquired via a 15-channel wireless headstage and receiver (W16; Triangle BioSystems). Analog signals were preamplified, digitized at a 24.414 kHz sampling rate (TB32; Tucker Davis Technologies, TDT), and fed via fiber optic link to an RZ5 base station (TDT) for filtering and processing. To reduce noise, the recordings from all but one channel (e.g. channels 2-15) were averaged together and subtracted from the remaining channel (e.g. channel 1). This method of common average referencing was applied to each channel individually (17). Offline, signals were high-pass filtered (300 Hz; 48 dB/octave roll-off), and a representative 16 sec recording segment was used to estimate the standard deviation (SD) of the background noise, using the algorithm described by Quiroga and colleagues (18). A spike extraction threshold was set 4-5 SDs above the noise floor, and an artifact rejection threshold was set to 20 SDs. Extracted spike waveforms were peak-aligned, hierarchically clustered, and sorted in principal component (PC) space using the MATLAB-based package UltraMegaSort 2000 (19) (Fig. S14). Single-units were characterized by clear separation in PC space, $\leq 10\%$ of spikes violating the refractory period, and $\leq 5\%$ spikes missing, as estimated from a Gaussian fit of the spike amplitude histogram (19) (Fig. S14). Recordings that did not meet these criteria were considered multi-units. Because of the small number of AM-responsive single-units in our dataset (see Table S1), we pooled single- and multi-units together for all group analyses reported here.

During behavioral recording sessions, the number of trials per session was unlimited, and AM depth values were adjusted within each session to maintain threshold bracketing (5). This approach allowed us to maximize our neurophysiological data collection each day.

Recordings were made both during task performance (the “engaged” condition), and during disengaged sessions that occurred just prior to (“pre”) and just after (“post”) the engaged sessions. The number of presentations for each warn depth (averaged across sessions) was

similar across listening conditions [pre: 16 ± 0.22; engaged: 16 ± 0.53; post: 15 ± 0.24; mean ± sem trials].

Neurometric Analysis

The firing rate (spikes/s) of each recording site was calculated over a 1 second duration for both unmodulated and AM noise. Firing rate-based d' values were calculated as:

$$d' = \frac{2\left(\mu FR_{AM} - \mu FR_{UNMOD}\right)}{\sigma FR_{AM} + \sigma FR_{UNMOD}} \quad (4)$$

where μFR_{AM} and σFR_{AM} are the mean and standard deviation of the firing rate for a single modulation depth, and μFR_{UNMOD} and σFR_{UNMOD} represent the mean and standard deviation of the firing rate elicited by the unmodulated noise.

Neural d' values were fit with a logistic function using a nonlinear least-squares regression procedure using the MATLAB function *nlinfit* (Mathworks) (16). The formula for this function is as follows:

$$F(x) = y_0 + \frac{a}{1 + \exp\left(-\left(x - x_0\right)/b\right)} \quad (5)$$

Here, y_0 represents the minimum d' value, x the modulation depth, a the range of d' values, x_0 the modulation depth at the inflection point, and b the slope of the function. The validity of each fit was assessed by calculating the statistical significance of the correlation (Pearson's r) between predicted and actual d' values. For each neurometric fit, threshold was defined as the

AM depth at which $d' = 1$. Units were considered responsive to AM stimuli if they generated a valid neurometric fit and threshold. Units were considered unresponsive if either (i) the fit was deemed invalid, or (ii) the highest d' elicited was below a value of 1. For units with valid fits and a minimum d' value above 1, threshold was set to the lowest AM depth presented in the session.

Cannula Implantation Surgery

Surgical procedures for cannula implantation were similar to those for electrode implantation, described above. After exposing and drying the skull, bone screws were inserted into both frontal bones. Craniotomies were made in the both parietal bones, dorsal and medial to each auditory cortex. Double guide cannula (26 gauge, 3 mm cannula length, 1.2 mm center-to-center distance; C235GS-5-1.2/SPC; Plastics One) were angled 20 degrees in the mediolateral plane. The mediolateral angle of electrodes and cannulas differed because the size of the cannulas prevented bilateral implants angled at 25 degrees. However, histology confirmed that our infusions were centered within ACx (Fig. S9). The rostral most cannula in each hemisphere was positioned 3.9 mm rostral and 4.8 mm lateral to lambda. Cannulas were inserted into left and right core auditory cortices, and the apparatus was secured to the skull via dental acrylic. Dummy cannulas (33 gauge, 3.2 mm cannula length, C235DCS-5/SP; Plastics One) were inserted to keep guides clear and were secured in place with a brass dustcap (303DC/1B; Plastics One). Animals were allowed to recover for at least 1 week before being placed on controlled water access.

Cannula Infusions

Muscimol (AbCam) was dissolved in 0.9% NaCl to achieve a concentration of 4 mg/mL. Aliquots (20-30 μL) were stored at -20°C and used within 1 week. Prior to infusions, aliquots were thawed to room temperature and diluted to 1 (Fig. S1) or 0.5 mg/mL (Fig. 4 and Fig. S11-12) with 0.9% NaCl.

Animals (n = 7 males) were anesthetized with isoflurane/O_2. Dust caps and dummy cannulas were removed from the guides. Infusion cannulas (33 gauge, 4 mm cannula length, C235IS-5/SP; Plastics One) were connected to PE-50 tubing (A-M Systems), backfilled with mineral oil, and connected to glass syringes (10 μL, 1801 Gastight, Hamilton) via 23s gauge needles (Hamilton). Muscimol or saline was drawn into the tip of each infusion cannula, and inserted into the guides. Bilateral infusions (1 μL/hemisphere, 0.2 μL/min) were made simultaneously using a six-channel programmable pump (NE-1600, New Era). Infusion success was confirmed by visually monitoring the movement of the meniscus between the infusion solution (muscimol or saline) and the mineral oil. To ensure full diffusion of the solution, infusion cannulas were left in place for 4 minutes before replacing dummy cannulas and caps. The entire process (from anesthesia induction to cap replacement) took 10-12 minutes. Animals recovered in their home cage for 45 minutes prior to behavioral training or testing. During this time, we observed animals to verify that they were alert and engaged, displayed proper posture, and demonstrated normal motor functions. One of the seven animals did not meet these criteria, and was therefore removed from the study. This animal was the smallest of the infusion group (55.5 gm), weighing >1.5 standard deviations below the mean of the remaining animals (69.5 +/- 8.7 gm).

The 6 remaining animals were used to determine whether ACx activity is necessary for PL (Fig. 4A-D and Fig. S11). Four of these animals were also used to determine whether ACx is necessary for detection of fully modulated AM noise (Fig. S1 and Fig. S10). These latter

experiments took place immediately after associative training was completed, prior to any psychometric training or testing.

When determining whether ACx was required for AM depth detection (Fig. S1), the warn stimulus (0 dB re: 100% depth) was presented a maximum of 20 times per session. During experiments exploring whether ACx activity is necessary for PL (Fig. 4, Figs. S11-S12), each depth was presented a maximum of 10 times. Given enough time or practice, animals with inactivated or lesioned brain regions may develop compensatory neural strategies to solve perceptual tasks (20, 21). In pilot experiments, we found that limiting sessions to 50 total trials minimizes compensation (not shown).

Histology

At the end of all experiments, animals were deeply anesthetized with an intraperitoneal injection of sodium pentobarbital (150 mg/kg) and perfused with phosphate-buffered saline and 4% paraformaldehyde. To mark recording sites in electrode-implanted animals, electrolytic lesions were made by passing current (7 mA, 10 sec) through one contact immediately before perfusion. To estimate the spread of muscimol diffusion in cannula-implanted animals, animals were infused with Fluoro-Ruby (10,000 MW Tetramethylrhodamine dextran, Thermo Fisher; 1μL /hemisphere) 30 – 90 minutes before perfusion. Brains were post-fixed and sectioned at 60 μm on a benchtop vibratome (Leica). Alternate sections from cannula-implanted animals were cleared and coverslipped for fluorescent imaging. All other sections were stained for Nissl. Brightfield and fluorescent images were acquired at 2X and 10X using a high-resolution slide scanner (Olympus). To verify recordings and infusions targeted core auditory cortex, electrode

tracks (Fig. S13) and dye spread (Fig. S9) were reconstructed offline and compared to a gerbil brain atlas (22).

Statistical Analysis

Statistical analyses were performed using JMP 9.0.1 (SAS), PASW Statistics 18.0, or SPSS Statistics 24.0. For normally distributed data (as assessed by the Shaprio-Wilk test), data are reported as mean ± sem unless otherwise stated. When data were not normally distributed, non-parametric analyses were used. In instances of multiple comparisons, alpha values were Holm-Bonferroni-corrected. When violations of sphericity were present, *P* values and degrees of freedom were Greenhouse-Geisser corrected.

For our physiology experiments, animals received perceptual training for either 5, 7, 10, or 14 days (each $n = 1$). We therefore restricted our group analyses to the first 7 days of training for which we had data from $n = 3$ animals. When performing within-subject analyses (such as in Fig. 1F-G, Fig. 3D-E, and Fig. S5), we used all data available. To quantify the correlation between neural and behavioral thresholds within individual animals (Fig. 1G, Fig. 3E and Table S2), we calculated Pearson's *r* and its associated *P* value.

The electrode position within each animal was advanced or kept steady based on the quality and number of AM-responsive recording sites on a given day. As a result of this approach, some sites were recorded over multiple training days, and other sites were only recorded on a single day. Thus, to quantify the overall effect of training on neural thresholds we chose to treat each recording site independently. We therefore used standard 1-way (non repeated-measures, RM) ANOVAs to analyze the neural data depicted in Fig. 1H, Fig 3F, Fig. S5 and Fig. S8.

To assess the effect of training on behavioral thresholds and false alarm rates (Fig. 1H and Fig. S4B), we performed two tests. First, missing values from one animal on days 6 and 7 prevented us from performing RM-ANOVAs for all 7 training days; thus, we performed 1-way RM-ANOVAs across only the first 5 days. Second, we performed less sensitive 1-way (non RM) ANOVAs for all 7 days of testing. As similar effects of training day were found for both tests, we only report the values for the RM-ANOVAs.

Similarly, because AM depths were systematically adjusted to maintain threshold bracketing (see Psychometric Training and Testing, above) some AM depth values were not presented on every test day. These missing values prevented us from performing RM-ANOVAs to test the effect of test day on hit rates (Fig. S4A). We therefore performed 1-way (non RM) ANOVAs for each stimulus value.

To calculate the rate of neural and behavioral improvement, we plotted data on an *x*-log scale, and fit data with a linear regression using the MATLAB functions *polyfit* and *polyval*. The slopes of these lines were taken as our measure of rate of improvement (Fig. 1H and Fig 3F).

To compare thresholds across days within individual units (Fig. 1I and Table S3), we used Student's paired two-tailed *t*-tests.

Because FRs were non-normally distributed, we used Kruskal-Wallis tests to analyze the effect of perceptual training on FR (Fig. S6A), FR standard deviations (Fig. S6B), FR ratios (Fig. 2B), and CV (Fig. 2C). We used the Friedman test and Wilcoxon Signed Ranks tests to compare firing rates across listening conditions (Fig. 3C).

We used a 1-way RM-ANOVA and Student's paired two-tailed *t*-tests to compare neural thresholds between disengaged (pre and post) and engaged listening conditions (Fig. 3B).

To examine the effect of a high dose of muscimol on detection of fully modulated (0 dB re: 100% depth) noise (Fig. S1), we used a 1-way RM-ANOVA. Post-hoc comparisons were performed with Student's paired two-tailed *t*-tests. To determine whether the effect of muscimol on 0 dB AM detection was dose-dependent (Fig. S10), we performed Student's paired two-tailed *t*-tests.

To determine whether a low dose of muscimol affected psychometric performance during training (Fig. S11), we performed a 2-way (stimulus x condition) RM-ANOVA. To determine whether muscimol infusions impaired PL, we examined the effect of time point (baseline, day 7, final) on behavioral *d'* values (Fig. 4C and 4E). Because we maintained threshold bracketing (see Psychometric Training and Testing, above), some AM depth values were not presented at every time point. We took two approaches to analyze data with missing values. First, we created restricted datasets by removing any AM depth value for which we had missing data. Second, we created complete datasets by filling in missing points with *d'* values extrapolated from the psychometric fitted functions. We then analyzed both the restricted and complete datasets using 2-way (time point x AM depth) RM-ANOVAs. Because these analyses yielded qualitatively similar results, we report only the test-statistics and *P* values from the analysis of the complete datasets here. We also used 2-way RM-ANOVAs to determine the effect of time point on thresholds obtained at 4 different *d'* cuts (1, 1.5, 2 and 2.5; Fig 4D and 4F).

To verify that muscimol-induced disruptions of PL were not due to task-specific impairments (such as reduced motivation or disrupted motor function) we examined the effect of ACx infusions on the rate of trial completion, false alarm rates, and reaction times using 1-way RM-ANOVAs (Fig. S12).

References

1. Heffner HE, and Heffner RS (1995) in *Methods in comparative psychoacoustics*, editor Klmup GM, Dooling RJ, Fay RR, and Stebbins WC (Springer, Basel, Switzerland), p 79-93.

2. Sarro EC, and Sanes DH (2010) Prolonged maturation of auditory perception and learning in gerbils. *Dev Neurobiol* 70:636-48.

3. Sarro EC, and Sanes DH (2011) The cost and benefit of juvenile training on adult perceptual skill. *J Neurosci* 31:5383-91.

4. Sarro EC, von Trapp G, Mowery TM, Kotak VC, and Sanes DH (2015) Cortical Synaptic Inhibition Declines during Auditory Learning. *J Neurosci* 35:6318-25.

5. Caras ML, and Sanes DH (2015) Sustained Perceptual Deficits from Transient Sensory Deprivation. *Journal of Neuroscience* 35:10831-10842.

6. Wakefield GH, and Viemeister NF (1990) Discrimination of modulation depth of sinusoidal amplitude modulation (SAM) noise. *J Acoust Soc Am* 88:1367-73.

7. Mogil JS (1999) The genetic mediation of individual differences in sensitivity to pain and its inhibition. *Proc Natl Acad Sci U S A* 96:7744-51.

8. Viemeister NF (1979) Temporal modulation transfer functions based upon modulation thresholds. *J Acoust Soc Am* 66:1364-80.

9. Buran BN, Sarro EC, Manno FA, Kang R, Caras ML, and Sanes DH (2014) A sensitive period for the impact of hearing loss on auditory perception. *J Neurosci* 34:2276-84.

10. Schütt HH, Harmeling S, Macke JH, and Wichmann FA (2016) Painfree and accurate Bayesian estimation of psychometric functions for (potentially) overdispersed data. *Vision Res* 122:105-23.

11. Green DM, and Swets JA (1966) *Signal Detection Theory and Psychophysics* (Wiley, New York).

12. Heffner HE, and Heffner RS (1984) Temporal lobe lesions and perception of species-specific vocalizations by macaques. *Science* 226:75-6.

13. Jamison HL, Watkins KE, Bishop DV, and Matthews PM (2006) Hemispheric specialization for processing auditory nonspeech stimuli. *Cereb Cortex* 16:1266-75.

14. Wetzel W, Ohl FW, and Scheich H (2008) Global versus local processing of frequency-modulated tones in gerbils: an animal model of lateralized auditory cortex functions. *Proc Natl Acad Sci U S A* 105:6753-8.

15. Buran BN, von Trapp G, and Sanes DH (2014) Behaviorally gated reduction of spontaneous discharge can improve detection thresholds in auditory cortex. *J Neurosci* 34:4076-81.

16. von Trapp G, Buran BN, Sen K, Semple MN, and Sanes DH (2016) A Decline in Response Variability Improves Neural Signal Detection during Auditory Task Performance. *J Neurosci* 36:11097-11106.

17. Ludwig KA, Miriani RM, Langhals NB, Joseph MD, Anderson DJ, and Kipke DR (2009) Using a common average reference to improve cortical neuron recordings from microelectrode arrays. *J Neurophysiol* 101:1679-89.

18. Quiroga RQ, Nadasdy Z, and Ben-Shaul Y (2004) Unsupervised spike detection and sorting with wavelets and superparamagnetic clustering. *Neural Comput* 16:1661-87.

19. Hill DN, Mehta SB, and Kleinfeld D (2011) Quality metrics to accompany spike sorting of extracellular signals. *J Neurosci* 31:8699-705.

20. Depner M, Tziridis K, Hess A, and Schulze H (2014) Sensory cortex lesion triggers compensatory neuronal plasticity. *BMC Neurosci* 15:57.

21. Kato HK, Gillet SN, and Isaacson JS (2015) Flexible Sensory Representations in Auditory Cortex Driven by Behavioral Relevance. *Neuron* 88:1027-39.

22. Radtke-Schuller S, Schuller G, Angenstein F, Grosser OS, Goldschmidt J, and Budinger E (2016) Brain atlas of the Mongolian gerbil (Meriones unguiculatus) in CT/MRI-aided stereotaxic coordinates. *Brain Struct Funct* 221 Suppl 1:1-272.

23. Fritz J, Shamma S, Elhilali M, and Klein D (2003) Rapid task-related plasticity of spectrotemporal receptive fields in primary auditory cortex. *Nat Neurosci* 6:1216-23.

24. Fritz JB, Elhilali M, and Shamma SA (2005) Differential dynamic plasticity of A1 receptive fields during multiple spectral tasks. *J Neurosci* 25:7623-35.

25. Fritz JB, Elhilali M, and Shamma SA (2007) Adaptive changes in cortical receptive fields induced by attention to complex sounds. *J Neurophysiol* 98:2337-46.

26. McGinley MJ, Vinck M, Reimer J, Batista-Brito R, Zagha E, Cadwell CR, Tolias AS, Cardin JA, and McCormick DA (2015) Waking State: Rapid Variations Modulate Neural and Behavioral Responses. *Neuron* 87:1143-61.

27. Goris RL, Movshon JA, and Simoncelli EP (2014) Partitioning neuronal variability. *Nat Neurosci* 17:858-65.

28. Kleinfeld D, Sachdev RN, Merchant LM, Jarvis MR, and Ebner FF (2002) Adaptive filtering of vibrissa input in motor cortex of rat. *Neuron* 34:1021-34.

29. Rosen MJ, Semple MN, and Sanes DH (2010) Exploiting development to evaluate auditory encoding of amplitude modulation. *J Neurosci* 30:15509-20.

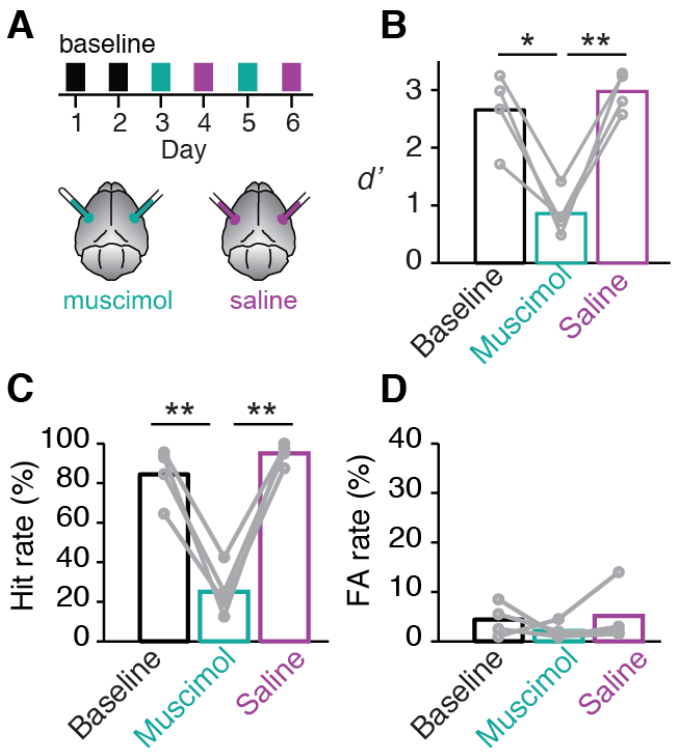

Fig. S1. Auditory cortex activity is necessary for AM detection

(A) Animals (n = 4) were implanted with cannulas into bilateral auditory cortex, and tested on their ability to detect fully modulated (0 dB re: 100%) AM noise using the task schematized in Fig. 1A. (Note that these animals were not implanted with chronic electrode arrays for wireless recording.) After 2 days of baseline testing, animals received bilateral infusions (1µL/hemisphere) of either a high dose of muscimol (1mg/mL; total dose of 2 µg) or saline on alternate days. **(B)** Muscimol impairs AM detection [$F_{2,6}$ = 33, P = 0.0006, n = 4; muscimol vs. baseline: t_3 = 5.6, P = 0.012; muscimol vs. saline: t_3 = 9.2, P = 0.0027]. Each point represents the average of two test days. Data from the same animal are connected by lines. Bars represent means. **(C)** Impairments were caused by reduced hit rates [$F_{2,6}$ = 69, P <0.0001; muscimol vs. baseline: t_3 = 7.7, P = 0.0045; muscimol vs. saline: t_3 = 10, P = 0.0019]. **(D)** Muscimol does not affect false alarm rates [$F_{2,6}$ = 0.50, P =0.63].

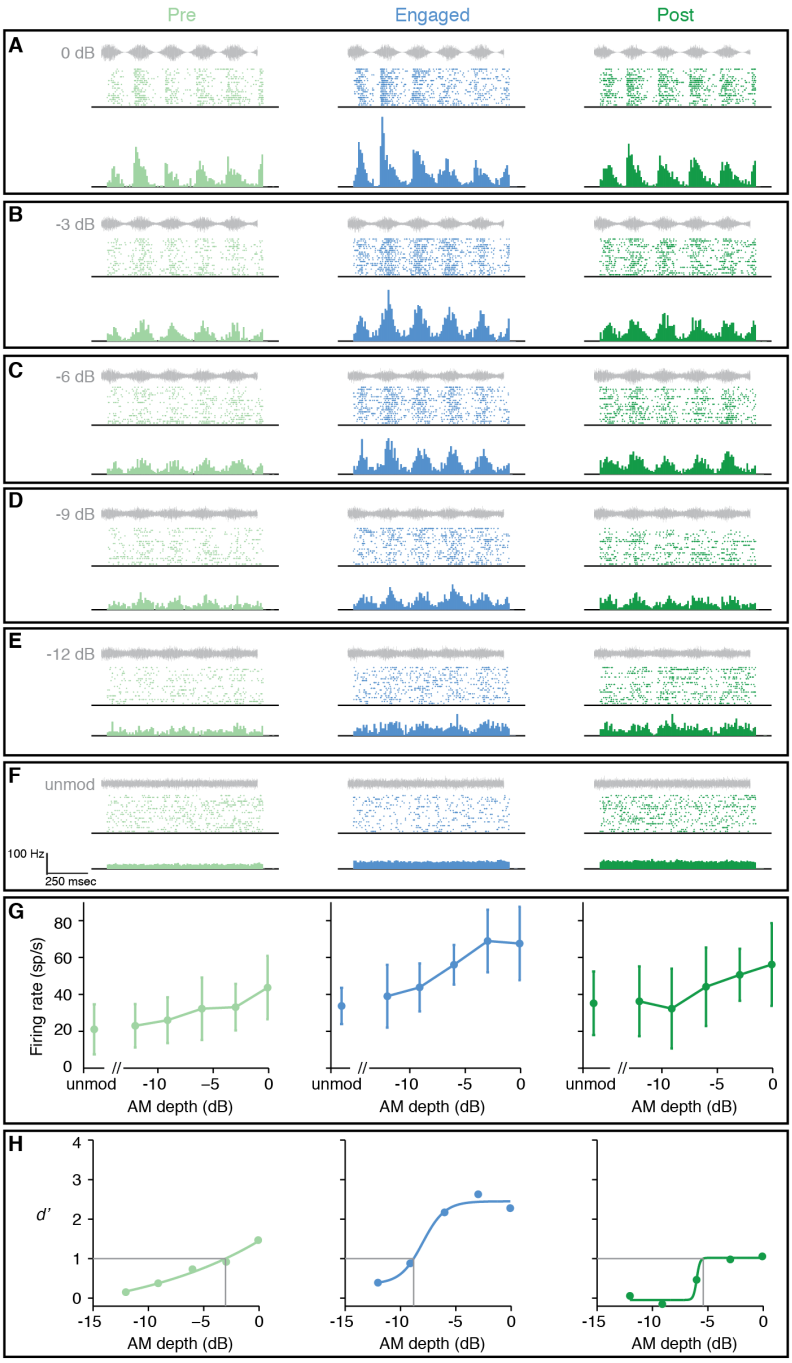

Fig S2. AM-driven activity is enhanced during task-engagement

(A-F) Rasters and post-stimulus time histograms (PSTHs) show AM-driven activity from one representative multi-unit in response to a range of AM depth stimuli. Responses were recorded on the first day of perceptual training. Grey waveforms show envelope of AM stimulus. Data are

from the same unit depicted in Fig. 3A. **(G)** The firing rate of this unit (mean ± stdev) is plotted as a function of AM depth. **(H)** The firing rate of this unit is transformed into the signal detection metric, *d'*, and plotted as a function of AM depth. Despite yielding valid thresholds during pre, engaged, and post conditions (grey lines in **H**), AM-driven activity in this unit is stronger during the engaged condition compared to the disengaged (pre and post) conditions, leading to enhanced sensitivity during task-engagement. Increased discharge rates and enhanced AM sensitivity appear to persist to some degree after task-engagement. A similar trend can be observed for the group data in Fig. 3F. This observation is consistent with previous reports of task-related ACx plasticity being maintained for hours after task completion (23-25).

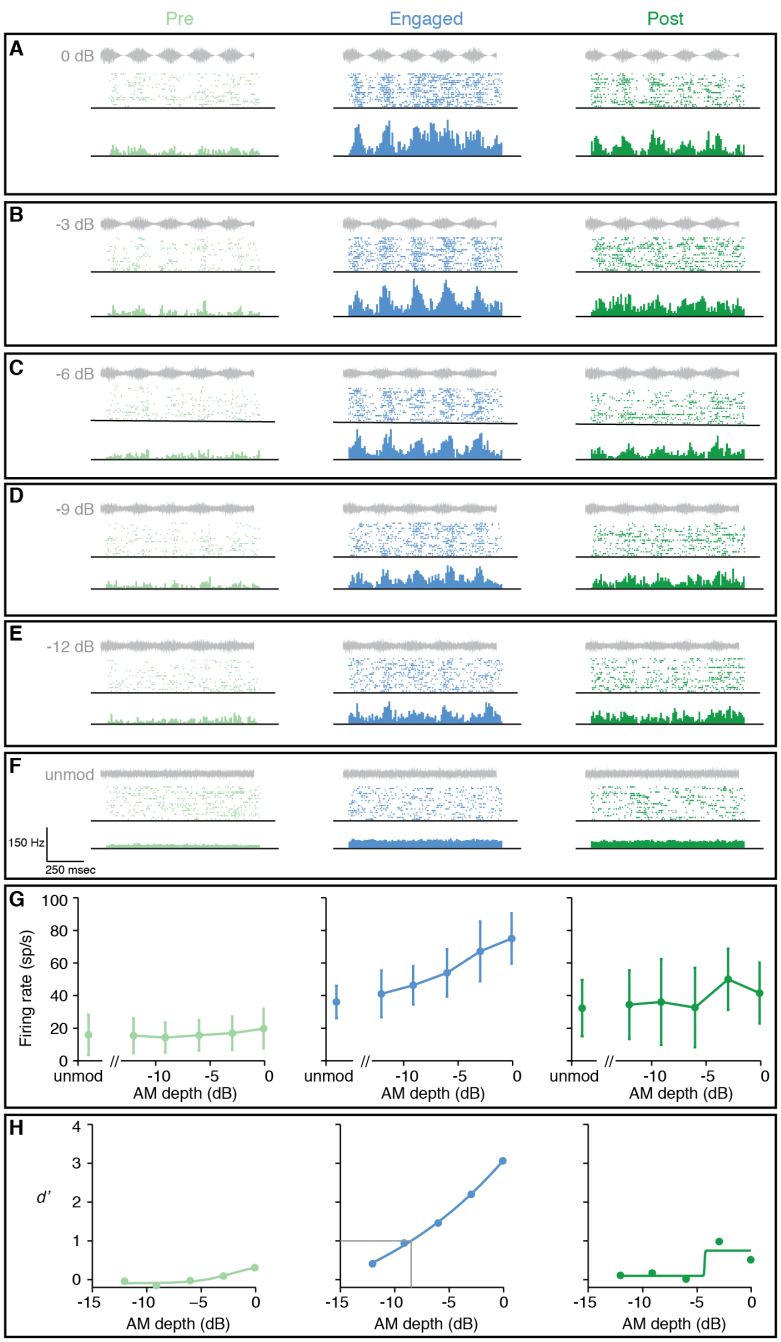

Fig S3. AM-driven activity is enhanced during task-engagement

Rasters and PSTHs (**A-F**), firing rates (**G**) and *d'* values (**H**) from another representative multi-unit from the first day of perceptual training. Plot conventions as in Fig. S2. This unit only yielded a valid threshold during task-engagement, and was therefore considered "unresponsive" to AM during pre and post conditions.

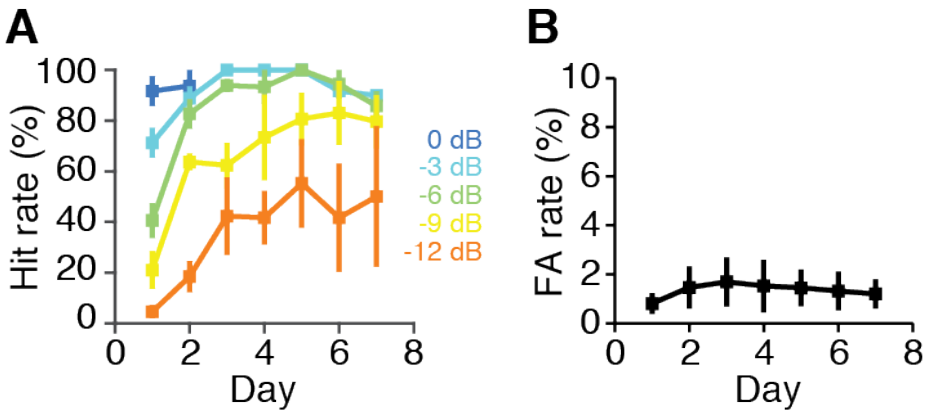

Fig. S4 Behavioral improvement is driven by increased hit rates

(A) Perceptual training increases hit rates [-3dB: $F_{6,10} = 5.3$, $P = 0.011$, $n = 4$ (days 1-3), 2 (day 4) and 1 (days 5-7); -6 dB: $F_{6,17} = 17.2$, $P < 0.0001$, $n = 4$ (days 1-3 and 5), 3 (days 4 and 6), 2 (day 7) ; -9 dB: $F_{6,19} = 4.2$, $P = 0.0075$, $n = 4$ (days 1-5), 3 (days 6-7); -12 dB: $F_{6,19} = 1.55$, $P = 0.22$; $n = 4$ (days 1-5), 3 (days 6-7)]. Note that because AM depths were systematically decreased to maintain threshold bracketing, 0 dB was only presented on the first two days. Therefore, no statistical test was performed for this stimulus value. **(B)** False alarm rates remain low throughout training [$F_{4,12} = 0.28$, $P = 0.88$; $n = 4$ animals].

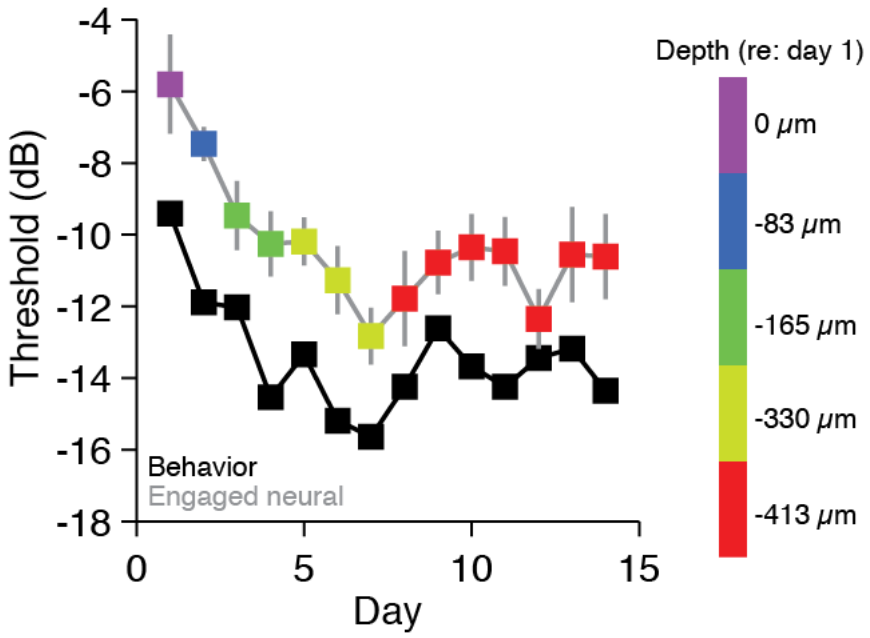

Fig. S5 Neural improvement is maintained after learning

Neural and behavioral sensitivity from one animal across 2 weeks of perceptual training. Neural thresholds improve during the first 7 days of training [Days 1-7: $F_{6,42} = 6.0$, $P = 0.0001$, $n = 49$ sites (range: 6-9/day)], and remain low during asymptotic perceptual performance [Days 7-14: $F_{7,42} = 0.81$, $P = 0.58$, $n = 50$ sites (range 4-8/day)]. Color indicates depth at which physiological data were recorded, relative to the starting depth on day 1. See Fig. S13 for histology from this same animal.

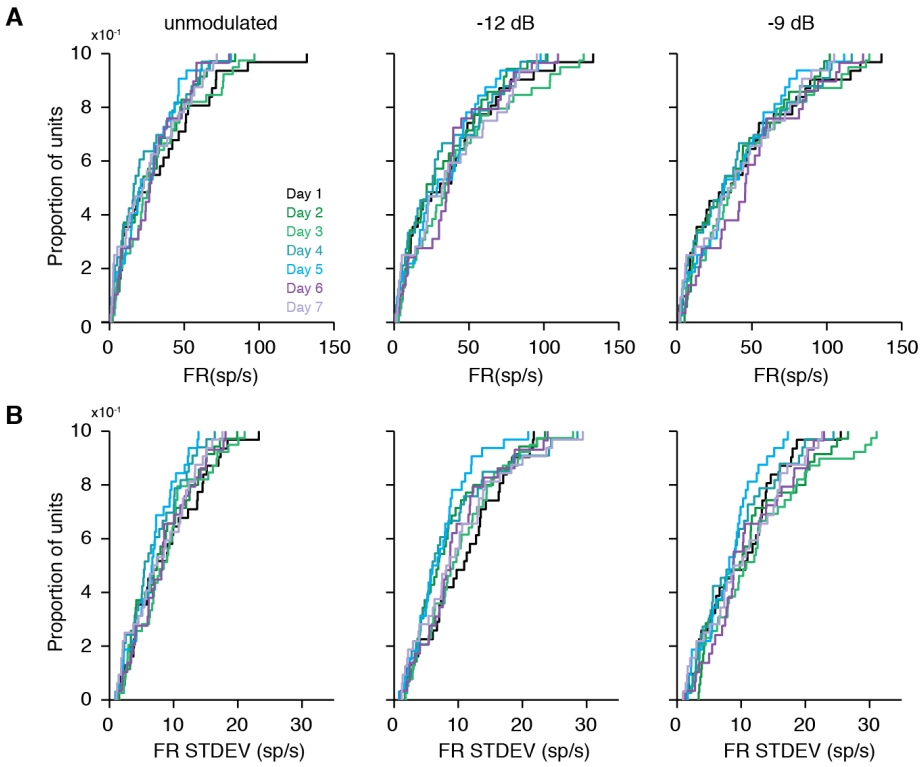

Fig. S6 Perceptual training does not affect FRs or FR STDEVs across the ACx population

(A) Population FRs do not change across training day [unmodulated: $H = 2.90$, $P = 0.821$; -12 dB: $H = 2.52$, $P = 0.866$; -9 dB: $H = 2.22$, $P = 0.899$]. **(B)** FR standard deviations also stay steady during training [unmodulated: $H = 4.58$, $P = 0.599$; -12 dB: $H = 7.82$, $P = 0.252$; -9 dB: $H = 5.52$, $P = 0.479$]. All $n = 231$ sites (range: 29-39/day; Table S1). The fact that the FR ratios of individual units increase throughout training (Fig. 2B) without a change in the global FR suggests that the day-to-day FR changes of individual units offset one another. As an example, in Fig. 2A, the FR distributions gradually separate from one another, but the day-to-day absolute FRs fluctuate in a seemingly random manner (i.e. compare where the Day 2 and Day 4 distributions fall along the *x*-axis in Fig. 2A). This finding suggests that two independent mechanisms simultaneously modulate FRs: one mechanism, induced by perceptual training,

enhances AM detection by increasing the separation of the warn and safe FR distributions. The second mechanism changes the daily FR gain on a unit-by-unit basis, in a stimulus-independent manner, possibly due to fluctuations in arousal, attention, or motivation (26, 27).

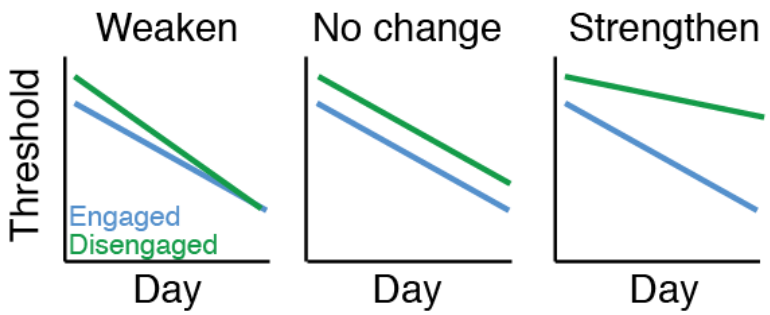

Fig. S7 Possible effects of training on a top-down process

The difference between engaged and disengaged neural thresholds reflects the strength of a top-down process. If training has no effect on this process, we would expect the magnitude of the engaged-disengaged difference to stay the same across days, despite training-based improvement (middle panel). Alternatively, if training weakens the top-down process, we would expect that the engaged-disengaged difference would gradually decrease across days (left panel). Finally, if training strengthens the top-down process, we would expect the engaged-disengaged difference to grow larger across days (right panel).

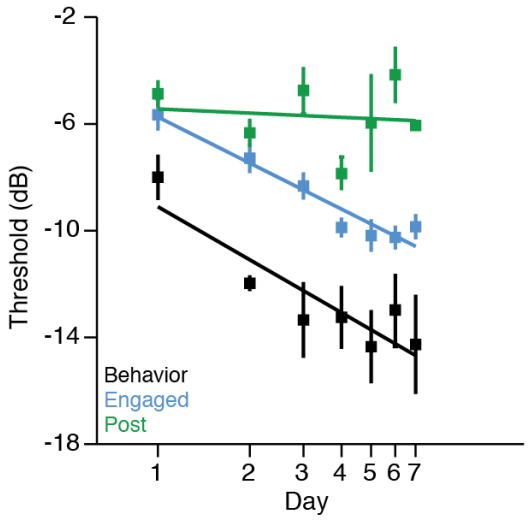

Fig S8. Behaviorally-gated neural improvement is observed using a timing-based analysis

Power was calculated from a discrete Fourier transform of spike times using a multitaper method using the Chronux toolbox for MATLAB (28, 29). This approach quantifies the magnitude of the discharge rate at the modulation rate of the AM stimulus (spikes/sec^2/Hz). As power includes both temporal and rate information in its calculation, but does not depend on stimulus phase-locking, it is a reasonable indicator of how well neural activity matches the shape of the stimulus amplitude envelope. Power values were transformed to *d'*, fit with a logistic regression, and thresholds were extracted from the fitted functions at *d'* = 1. Power-based thresholds obtained during task-engagement improved throughout perceptual training [$F_{6,171} = 10.9$, $P < 0.0001$, $n =$ 178 sites (range 22-31/day); -5.7 dB/log(day)]. Power-based thresholds obtained during disengaged listening sessions immediately following task performance ("post") did not improve [$F_{6,14} = 2.40$, $P = 0.083$, $n = 21$ sites (range 1-6/day); -0.52 dB/log(day)]. Note that the effect of training could not be assessed on thresholds from disengaged listening sessions that occurred immediately prior to task performance ("pre") because only 2 training days yielded valid power-based thresholds from more than one site.

373 **Fig. S9 Estimated spread of muscimol**

374 Representative coronal section shows spread of Fluro-Ruby (1 μL/hemisphere) 45 minutes after

375 bilateral ACx infusion.

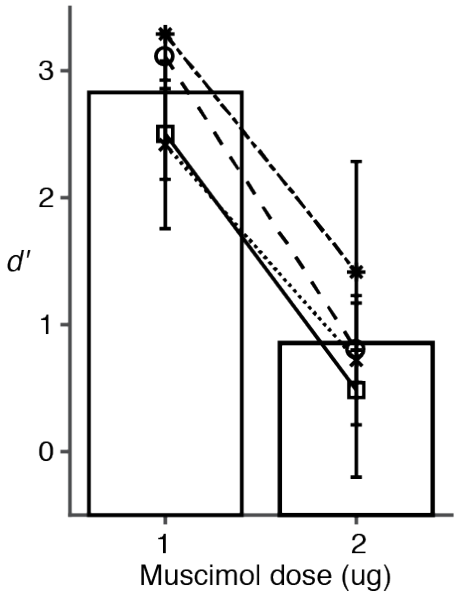

Fig S10. Dose-dependent effect of muscimol on AM detection

A high dose of muscimol (1μL/hemisphere; 1mg/mL; total dose of 2 μg) impairs detection of fully modulated (0 dB re: 100%) AM noise. A lower dose (1μL/hemisphere; 0.5 mg/mL; total dose of 1 μg) allows for excellent detection of 0 dB AM in the same animals (n = 4). Data from the same animal are connected by lines. The effect of dose was significant [t_3 = 15.29, P = 0.0006, n=4 animals]. Bars represent means. High dose (2 μg) data are replotted from Fig. S1, with each point representing the average of two muscimol sessions collected during associative testing (prior to perceptual training) on alternating days. Low dose (1 μg) data points represent the average of all *d'* values generated at 0 dB during perceptual training sessions paired with muscimol (i.e. Days 2-6 in Fig. 4A). Because AM depth values were adjusted daily to maintain threshold bracketing during perceptual training, animals were tested with 0 dB for a variable number of low-dose sessions (range: 2-4).

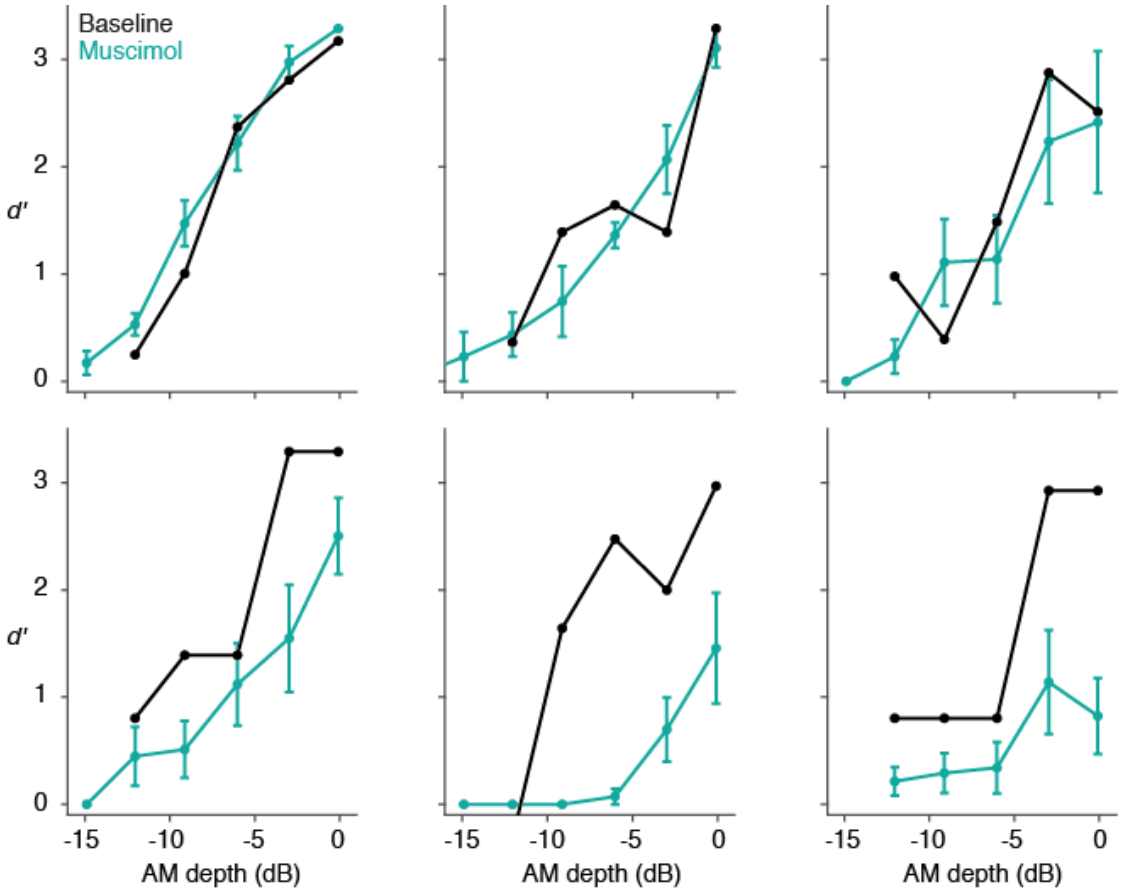

Fig S11. A low dose of muscimol does not grossly impair psychometric performance

Comparisons of psychometric performance at baseline and during muscimol training sessions. Each panel contains data from a single animal. Muscimol data are averaged across all muscimol training sessions (Days 2-6 in Fig. 4A). In general, a low dose of muscimol (0.5 mg/mL; 1μL/hemisphere; total dose of 1 μg) did not grossly perturb AM perception [$F_{1,5}$ = 5.14, P = 0.073, n = 6 animals], but did impair learning (see Fig. 4).

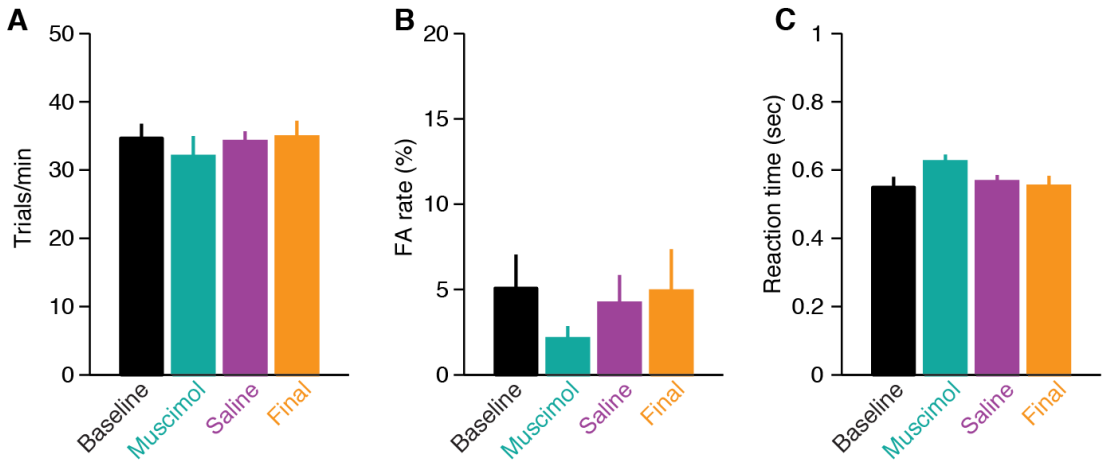

396 **Fig. S12 Muscimol-induced disruption of PL is not explained by task-specific impairments**

397 A low dose of muscimol (0.5 mg/mL, 1μL/hemisphere; total dose of 1 μg) does not affect (**A**)
398 the rate of trial completion [$F_{1.8,9.2} = 0.36$, $P = 0.69$], (**B**) false alarm rates [$F_{1.2,6.2} = 0.93$, $P =$
399 0.39], or (**C**) hit trial reaction times [$F_{3,15} = 2.2$, $P = 0.13$]. For muscimol and saline conditions,
400 across-session means were calculated for each animal. These mean values were then averaged
401 across animals to obtain the bars and sems depicted here. All $n = 6$ animals.

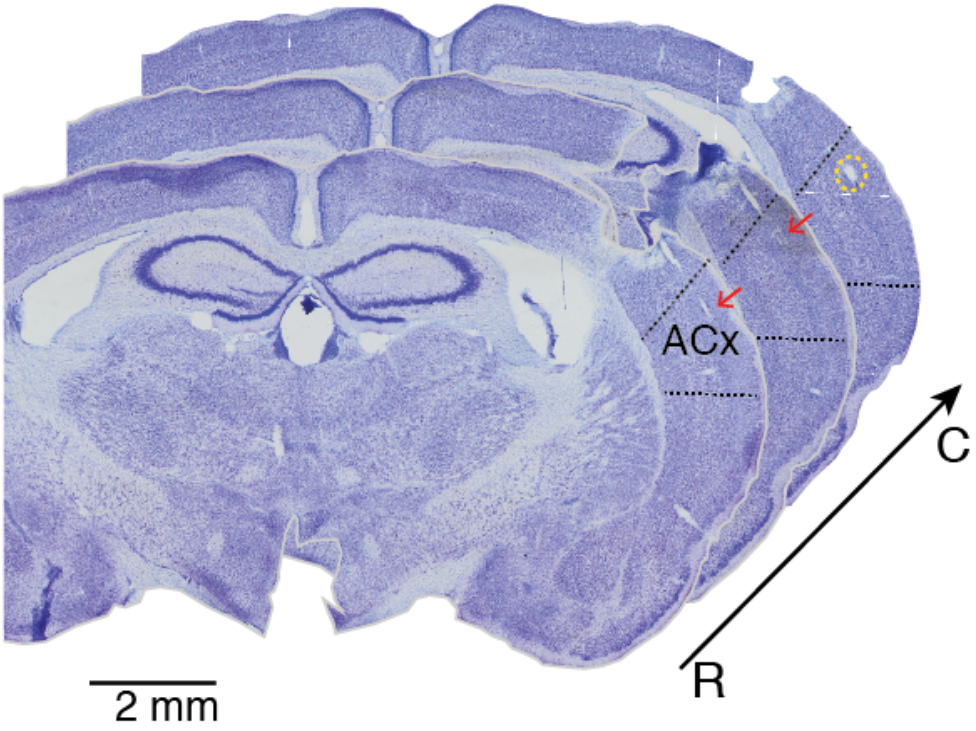

Fig. S13 Representative electrode track

Nissl-stained coronal sections from one animal arranged from rostral (R) to caudal (C) showing electrode tracks (red arrows) and electrolytic lesion (yellow circle) in ACx. Sections were separated by 180 μm.

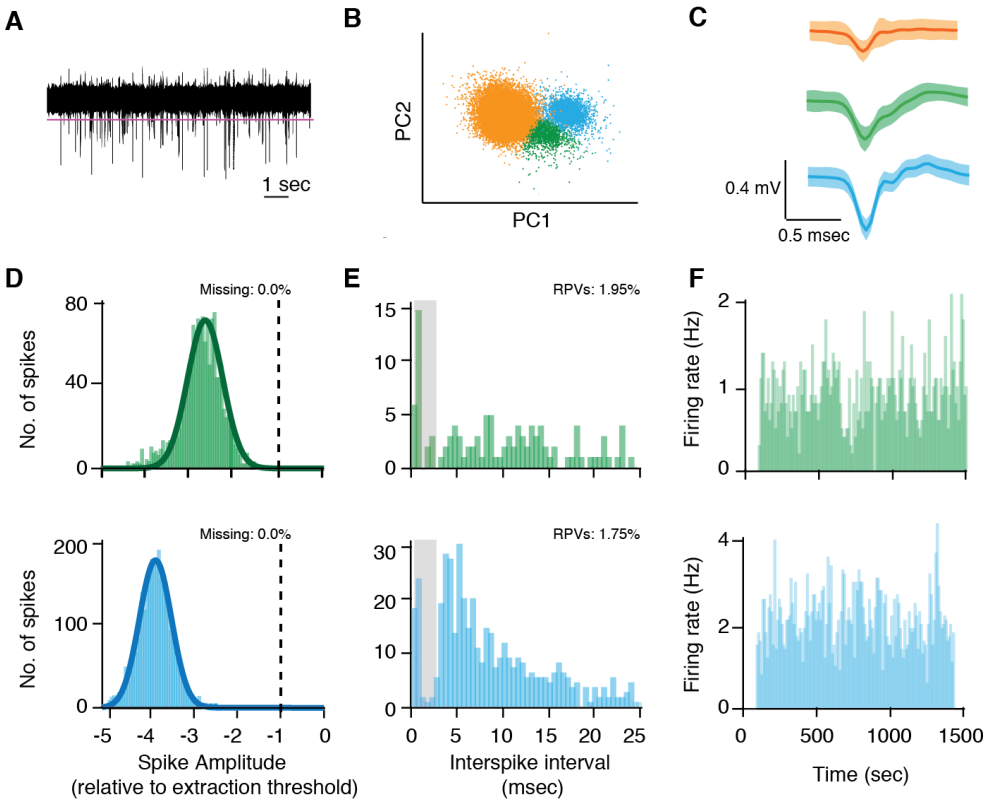

406 **Fig. S14 Spike sorting and single-unit verification**

407 **(A)** Representative voltage trace after filtering and common average referencing. Magenta line
408 indicates snippet extraction threshold. (**B**) Extracted snippets were sorted in principal component
409 (PC) space, generating **(C)** sorted waveforms (means ± 2 stdev). **(D)** Distribution of spike
410 amplitudes for the two single-units identified in **C**. Dashed vertical line represents amplitude of
411 extraction threshold. Thick line represents a Gaussian fit of the distribution, allowing for an
412 estimation of the percent of spikes missing. **(E)** Distribution of interspike-intervals for each
413 single-unit. Grey shading highlights refractory period. For both units < 2% of spikes were
414 refractory period violations (RPVs). **(F)** Firing rate histograms for each single unit over the
415 duration of the recording session. Both units show steady firing rates, demonstrating recording
416 stability.

Table S1.

Number of units responsive to AM, broken down by day and by session type.

	Pre		Engaged		Post	
Day	**Multi**	**Single**	**Multi**	**Single**	**Multi**	**Single**
1	11	0	29	2	11	1
2	6	0	32	3	5	0
3	11	0	37	2	14	0
4	4	0	33	0	7	0
5	6	0	29	3	7	0
6	2	0	28	1	4	0
7	3	1	30	2	6	0
Total	**43**	**1**	**218**	**13**	**54**	**1**

Table S2.

Within-animal correlations between behavioral and neural thresholds. AM responses during the Pre condition from subject 221955 were only observed on one day, so no correlation value could be calculated. *Significant after adjusting alpha level for multiple comparisons.

	Pre			Engaged			Post		
Subject ID	***r***	***P***	**slope**	***r***	***P***	**slope**	***r***	***P***	**slope**
217821	0.87	0.012	0.53	0.85	<0.0001*	0.74	0.39	0.23	0.32
221955	--	--	--	0.99	0.0014*	1.2	0.85	0.35	2.3
222724	0.87	0.052	1.6	0.61	0.14	0.93	0.65	0.16	1.7
222725	0.56	0.093	0.79	0.92	0.0002*	0.81	0.63	0.051	0.75

Table S3.

Within-site threshold comparisons during perceptual training (Student's paired two-tailed *t*-tests). Only units that yielded a valid threshold on both days were included in the analyses. Because some sites were lost during later sessions, the Day 1 thresholds (and the sample sizes) differ for each comparison. Data are from $n = 2$ animals. (We advanced the electrode in the remaining 2 animals throughout Days 1-5, making within-unit comparisons in those subjects impossible). *Significant after adjusting alpha level for multiple comparisons.

Comparison	Day 1 threshold (dB re: 100%) Mean ± SEM	Day N threshold (dB re: 100%) Mean ± SEM	*t*(df)	*P*	Effect size (Cohen's *d*)
Day 1 vs. Day 2	-7.0 ± 0.91	-9.9 ± 0.81	5.1(15)	0.0001*	0.65
Day 1 vs. Day 3	-6.8 ± 0.97	-9.0 ± 0.76	5.5(15)	<0.0001*	0.84
Day 1 vs. Day 4	-7.4 ± 0.99	-11 ± 0.81	8.3(13)	<0.0001*	1.2
Day 1 vs. Day 5	-7.5 ± 1.0	-13 ± 1.0	8.6(11)	<0.0001*	1.5

Table S4.

Chi-square analysis of the effect of listening condition (pre, engaged, post) on unit responsiveness to AM, broken down by day. See Table S1 for raw counts of responsive units. *Significant after adjusting alpha level for multiple comparisons.

	% Units Responsive to AM					
Day	**Pre**	**Engaged**	**Post**	**Pearson X^2**	**df**	***P***
1	23.9	67.4	26.1	23.2	2	<0.001*
2	13.0	74.5	10.6	55.6	2	<0.001*
3	20.0	69.6	25.9	34.4	2	<0.001*
4	8.50	68.8	15.2	48.3	2	<0.001*
5	12.2	65.3	14.6	41.2	2	<0.001*
6	5.00	70.7	10.0	53.0	2	<0.001*
7	9.30	71.1	14.0	48.2	2	<0.001*